J Mater Sci (2009) 44:1757–1763
DOI 10.1007/s10853-009-3286-1

Single crystal growth in PMN-PT and PMN-PZT

Thomas Richter · Carsten Schuh · Ender Suvaci · Ralf Moos

Received: 15 December 2008 / Accepted: 20 January 2009 / Published online: 18 February 2009

Abstract Single crystal growth of lead-based piezoelectric ceramics $Pb(Mg_{1/3}Nb_{2/3})_{0.68}Ti_{0.32}O_3$ (PMN-32PT) and $Pb(Mg_{1/3}Nb_{2/3})_{0.42}(Ti_{0.638}Zr_{0.362})_{0.58}O_3$ (PMN-37PT-21PZ) ceramics via templated grain growth (TGG) was investigated. (001)- and (111)-oriented $BaTiO_3$ (BT) single crystals and (001)-oriented $SrTiO_3$ (ST) single crystals (of approximately 2.5 × 2.5 × 1 mm) were utilized as seeds for the growth experiments. The piezoelectric single crystals were produced in a process that involves at first hot pressing of single crystal in cold isostatically pressed ceramics followed by subsequent sintering of the samples. Growth of (001)-oriented single crystals with BT seeds was observed in both PMN-32PT and PMN-37PT-21PZ matrices. The measured growth lengths were up to 140 and 65 μm, respectively. The grown (001)-oriented single crystals grown were rectangular. The measured growth lengths of the pyramidal-shaped (111) BT single crystals were up to 1 mm, which is much larger than the growth lengths of the (001) single crystals. Experiments on (001) ST-seeded single crystals were not successful. No single crystal growth was observed due to the dissolution of the ST single crystals in the PMN-PZT matrix. The differences were explained by defect-chemical considerations.

T. Richter (✉)
Powertrain, Continental AG, 93055 Regensburg, Germany
e-mail: Thomas.3.Richter@continental-corporation.com

C. Schuh
Ceramics Department, Siemens AG, Corporate Technology, Munich, Germany

E. Suvaci
Department of Materials Science and Engineering, Anadolu University, Eskisehir, Turkey

R. Moos
Functional Materials Laboratory, University of Bayreuth, 95447 Bayreuth, Germany

Introduction

It has been previously shown that piezoelectric single crystal PMN-35PT can exhibit a strain up to 0.5% [1] and a $d_{33} > 2000$ pm/V measured in the ⟨001⟩ direction [2]. These enhanced properties require a rhombohedral composition near the morphotropic phase boundary in the ⟨001⟩ direction [3].

Templated grain growth (TGG) is an established method to make single crystals of incongruent melting materials such as $Pb(Zr,Ti)O_3$ (PZT) [4]. In this process, a single crystalline template is placed in contact with a sintered polycrystalline matrix. The contact between the seed single crystal and the dense, fine-grained matrix is usually established by hot pressing. A subsequent sintering step allows the seed single crystal to grow into the matrix. The growth of the seed single crystals into fine-grained dense matrix occurs via liquid phase diffusion mechanisms.

PMN-PT compositions have been shown to be suitable for single crystal growth experiments using the TGG process [5–8]. Li et al. [9] used an (111)-oriented $SrTiO_3$ (ST) single crystal as seed and a PMN-32PT as matrix. They bonded the ST single crystal onto the polished surface of the hot pressed matrix, using a PbO-based interlayer. Single crystal growth of up to 2 mm was measured. The use of ST single crystals is crucial because of their dissolution into lead-based liquid phases [10]. $BaTiO_3$ (BT) is another seed composition that has been tested to date for the PMN-PT based systems. Sabolsky et al. [8] investigated the growth of (001)-oriented BT single crystals in a PMN-35PT matrix.

The advantage of BT single crystals over ST single crystals is their chemical stability. Single crystal growth of up to 120 μm was measured, and it was possible to fit the growth length to a cubic growth law.

On the other hand, this kind of single crystal growth causes certain problems. Khan et al. [1, 11] reported that pores are entrapped after hot pressing and sintering in air. Furthermore, the use of a PbO liquid phase leads to enclosed PbO in the grown single crystal. The consequence of these single crystal defects is an increased hysteresis of the strain versus electric field as mentioned by Khan et al. [1]. Gorzkowski et al. [6] investigated a method of preventing porosity within the matrix and the grown single crystal. They applied a vacuum during the preceding hot pressing step to achieve fully dense samples after sintering. Porosity is caused by slow-diffusing gases in the hot pressing atmosphere [12, 13]. Nitrogen, for example, is compressed during hot pressing and enclosed within the ceramic or within the single crystal. The subsequent sintering leads to a swelling of the nitrogen that causes increased porosity.

The aim of this work was to achieve single crystal PMN-32PT and PMN-37PT-21PZ via templated grain growth. BT and ST single crystals were used as seeds. The seed single crystals were approximately 2.5 × 2.5 × 1 mm and had one face polished. The seed single crystals grew into the matrix during the TGG. It is shown that single crystal growth length and quality depends on the sintering time, the orientation of the single crystal, the matrix composition, and the hot pressing atmosphere.

Experimental

In this study, $Pb(Mg_{1/3}Nb_{2/3})_{0.68}Ti_{0.32}O_3$ (PMN-32PT) and $Pb(Mg_{1/3}Nb_{2/3})_{0.42}(Ti_{0.638}Zr_{0.362})_{0.58}O_3$ (PMN-37PT-21PZ) ceramics were utilized as matrix compositions. PbO (Lindgens), TiO_2 (Treibacher), ZrO_2 (Treibacher) and $MgNb_2O_6$ (H.C. Starck) were used to prepare the powder. The stoichiometric oxides were mixed and subsequently high-energy milled. The mixed and milled oxide mixture was then freeze-dried. The dried oxide mixture of both compositions was calcined at 750 °C for 4 h, subsequently mixed with an additional lead oxide excess of 1.5 mol% and finally high-energy milled for a second time.

The (001)- and (111)-oriented $BaTiO_3$ (BT) and (001) $SrTiO_3$ (ST) single crystals with a size of 2.5 × 2.5 × 1 mm and one polished face were used as seed for single crystal growth. They were embedded in the matrix powder and then cold isostatically pressed at 300 MPa. Before single crystal growth, the pressed samples of PMN-32PT and PMN-37PT-21PZ were densified by hot pressing for 30 min at 45 MPa and 900 or 940 °C, respectively. Oxygen or air was used as the two hot pressing atmospheres. To inhibit PbO volatilization during subsequent single crystal growth, the samples were wrapped in platinum foil and embedded in PMN-32PT powder inside a closed double platinum crucible. All samples were heated at 15 °C/min and sintered in air at 1150 °C with sintering times varying from 0 to 10 h.

After single crystal growth, samples were cut perpendicular to the (001) or (111) single crystal orientation. Sintered samples were polished and thermally etched at 900 °C for 15 min. No grain growth occurred during thermal etching. The average length and the standard deviation of single crystal growth were determined from 50 measurements along the BT single crystal. The grain size was determined by measuring the equivalent spherical diameters (e.g., the diameter of a sphere with the same area as the respective grain) of at least 200 grains. The average diameter determined was multiplied by 1.24 to obtain the average grain size. The corrected average diameter describes the real grain size whereas the mentioned factor is calculated for this kind of grain size measurement. The density of hot pressed and sintered samples was measured by a He-pycnometer ("Accupyc", Micromeritics GmbH).

Results

After initial hot pressing, both PMN-32PT and PMN-37PT-21PZ matrices had a density of 8.1 g/cm^3, which was set to 100% theoretical density. The different atmospheres (air and oxygen) showed no influence on densification during hot pressing. The influence of the hot-pressing atmosphere was investigated by subjecting PMN-32PT to hot pressing in air and in oxygen and subsequent sintering. There was no change in the densities of the matrices when an oxygen atmosphere was applied during hot pressing. The density remained nearly constant at 8.1 g/cm^3 (Fig. 1). The influence of the atmosphere on density becomes visible after hot pressing in an air atmosphere. The density of PMN-32PT hot pressed in air, unlike the density of the same material hot pressed in an oxygen atmosphere, decreased during subsequent sintering (see Fig. 1). Density decreased to 98% merely after heating to the sintering temperature (1050 °C for 0 h). Sintering for a longer period produced a further decrease in density. This decrease in density is probably related to the nitrogen in air [12, 13]. The nitrogen is compressed during hot pressing and then swells during subsequent sintering.

Matrix grain growth behavior was investigated using PMN-32PT and PMN-37PT-21PZ during hot pressing in oxygen. Figure 2 illustrates the average grain size of both compositions as a function of sintering time at 950 and 1150 °C, respectively. Due to the different growth

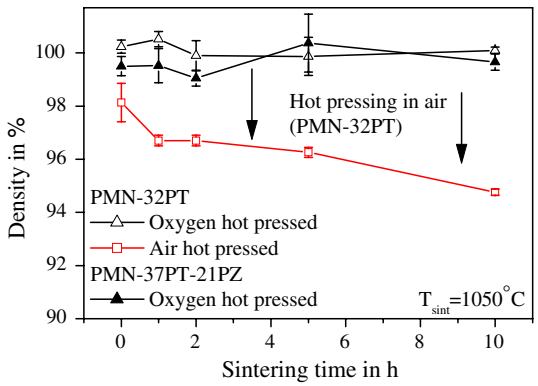

Fig. 1 Density of PMN-32PT (hot pressed in oxygen and in air) and PMN-37PT-21PZ (hot pressed in oxygen) as a function of sintering time at 1050 °C

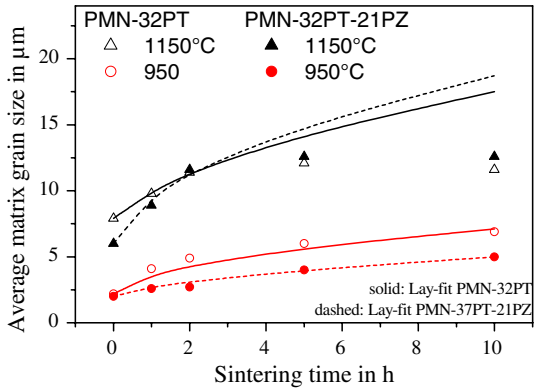

Fig. 2 Average matrix grain size of PMN-32PT and PMN-37PT-21PZ as a function of sintering time at 1150 and 950 °C; the *solid* and the *dashed lines* characterize the fit with the Lay model

mechanisms [1], abnormal grains were not included in the grain size measurements, since their number is very low (e.g., in the measured area only about five abnormal grains were counted). Furthermore, not all samples showed abnormal grains. The solid and dashed lines represent the Lay fit [14] of the grain size for the PMN-32PT and PMN-37PT-21PZ systems, respectively. The fit of the cubic growth law to the measured grain size is described in greater detail in the "Discussion" section. The average grain size for both matrices is 1.8 µm after hot pressing. During subsequent sintering, the average grain size for PMN-32PT and PMN-37PT-21PZ increased to 7 and 4.7 µm, respectively, after 10 h sintering at 950 °C. Grain size after 2 h sintering at 1150 °C increased to about 12 µm. As already described by Sabolsky et al. [8], longer sintering times did not lead to further grain growth.

Figure 3a and b shows the initial state for the single crystal growth experiments (after hot pressing and before sintering) of the (001)-oriented BT single crystals in PMN-32PT and PMN-37PT-21PZ matrices, respectively. It was made up from a hot pressed bulk sample including a centered single crystal. The hot pressed initial state is characterized by a fine-grained dense matrix and good contact between the seed single crystal and the matrix. The BT single crystal in the PMN-32PT matrix began to grow during hot pressing (Fig. 3a), but no single crystal growth was observed in the initial state of PMN-37PT-21PZ (Fig. 3b).

Single crystal growth experiments were performed at 1150 °C in air using the aforementioned initial state. Figure 4 shows that (001) and (111) single crystals of PMN-32PT were grown. The pores are caused by the use of an air atmosphere during hot pressing. The main differences between the (001)- and (111)-oriented BT single crystals are the shape and the growth length of the grown single crystals. (001)-oriented BT seed single crystals lead to the growth of rectangular-shaped PMN-32PT and PMN-37PT-21PZ single crystals. The measured single crystal growth lengths are shown in Fig. 5 and Table 1. The grown (001) BT single crystals had lengths of up to 140 µm for PMN-32PT and 65 µm for PMN-37PT-21PZ. The single crystal growth length is a function of the sintering time and will be described in more detail in the "Discussion" section. As can be seen in Fig. 4c and d, (111)-oriented BT seed single crystals lead to pyramidal-shaped PMN-32PT single crystals with growth lengths of up to 0.5 and 1 mm, depending on the hot pressing atmosphere (air or oxygen). Figure 6a shows an example of an EDX line scan of the

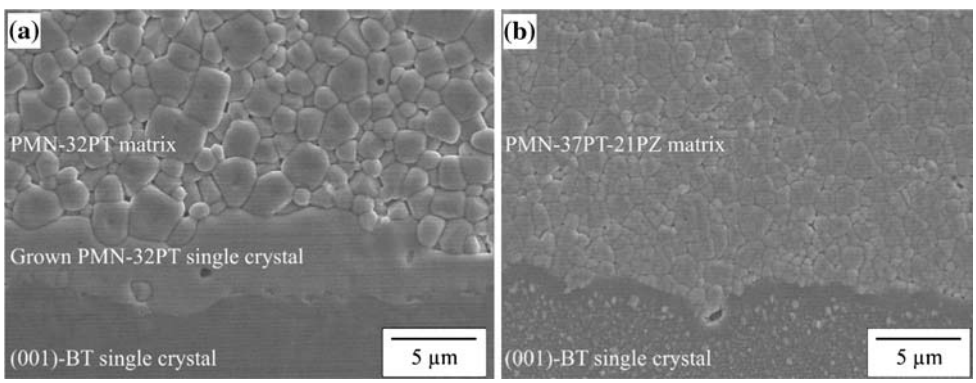

Fig. 3 Interface of BT single crystal and **a** the PMN-32PT matrix and **b** the PMN-37PT-21PZ matrix in the initial (hot pressed) state

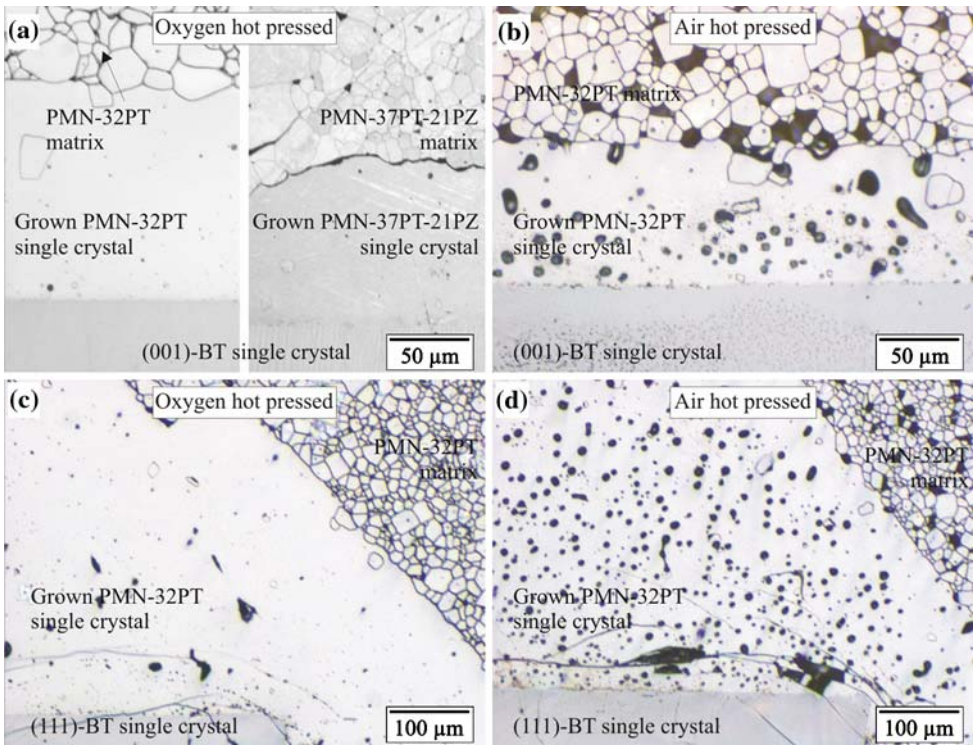

Fig. 4 Grown single crystalline PMN-32PT and PMN-37PT-21PZ, using seeds of (001)- and (111)-oriented BT single crystals at 1150 °C and 10 h. **a** (001) BT-oriented single crystal growth in both matrices (hot pressed in oxygen, *left*: PMN-32PT matrix, *right*: PMN-37PT-21PZ matrix). **b** (001) BT-oriented single crystal growth in the PMN-32PT matrix (hot pressed in air). **c** (111) BT-oriented single crystal growth in the PMN-32PT matrix (hot pressed in oxygen). **d** (111) BT-oriented single crystal growth in the PMN-32PT matrix (hot pressed in air)

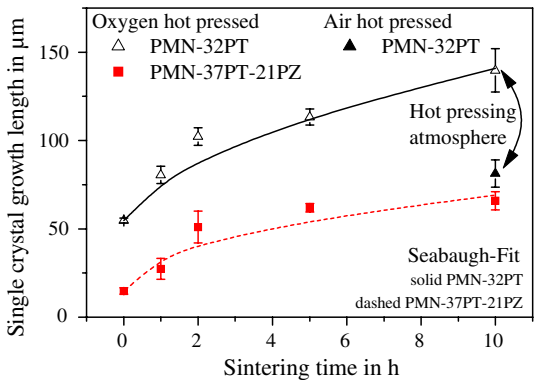

Fig. 5 Single crystal growth lengths of PMN-32PT (oxygen hot pressed and air hot pressed) and PMN-37PT-21PZ (oxygen hot pressed) at 1150 °C for different sintering times

interface between the (001)-oriented BT single crystal and the PMN-32PT matrix. As can be seen, the Ba and Pb content are constant. This means BT single crystals are stable in both matrices, as already reported by Sabolsky et al. [8].

The hot pressing atmosphere (air and oxygen), which was investigated in the PMN-32PT matrix and both BT single crystal orientations, is very important for single crystal growth during subsequent sintering. Hot pressing in air leads to enclosed porosity within the PMN-32PT single crystal grown (see Table 1). As can be seen in Fig. 4b and d, the size of the pores increases with increasing distance to the BT single crystal. The porosity resulted in a decreased single crystal growth rate as compared with the dense matrices (hot pressed in oxygen) and, hence, in a decreased single crystal growth length. Figure 5 shows the single crystal growth lengths of (001) BT single crystals in the dense (oxygen hot pressed) PMN-32PT and PMN-37PT-21PZ matrices and in the porous (air hot pressed) PMN-32PT matrix. The growth lengths after 10 h sintering time were 140 µm for oxygen hot pressed PMN-32PT and 81 µm for air hot pressed PMN-32PT. The same behavior was observed using (111) BT single crystals. The growth lengths measured were up to 1 and 0.75 mm for oxygen and air hot pressed PMN-32PT, respectively.

The (001) ST single crystals were used as alternative seed single crystals. The experiments showed (Fig. 6b) that no single crystal growth had occurred. Figure 6b also shows a superposed EDX line scan of Sr and Pb near the interface between the matrix and the seed single crystal. It can be seen that there is a gradual decrease in the Sr content and a gradual increase in the Pb content as the distance to the ST single crystal increases. This means that a Sr diffusion zone developed between the matrix and the ST single crystal. Even though a pre-sintering step at 700 °C was used, the ST single crystal was not chemically stable in the PMN-32PT matrix.

Discussion

The hot pressing atmosphere was found to be critical in order to achieve a dense matrix after sintering. The density of

Table 1 Determined growth constant K of matrix coarsening behavior and single crystal growth behavior

Temperature (°C)	K_3 (matrix) (m^3/s)		K_3 (single crystal) (m^3/s)	
	PMN-32PT	PMN-37PT-21PZ	PMN-32PT	PMN-37PT-21PZ
1150	1.3×10^{-19}	1.6×10^{-19}	7.3×10^{-17}	9.1×10^{-18}
950	9.5×10^{-21}	3.2×10^{-21}	–	–

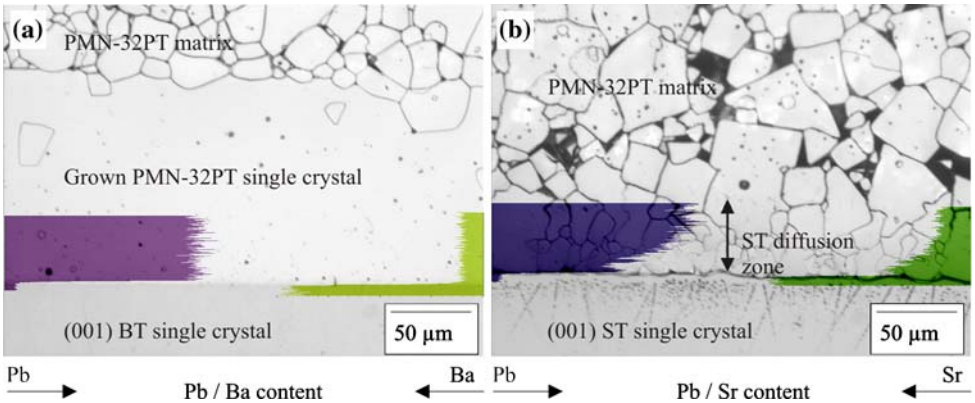

Fig. 6 EDX line scan of the interface between single crystals and the matrix sintered at 1150 °C for 10 h in oxygen. **a** (001) BT single crystalline seed. **b** (001) ST single crystalline seed

matrices, which have undergone a prior hot pressing in air, decreases during sintering due to the low diffusion velocity of entrapped gases [12, 13]. The slow-diffusing gas in air is nitrogen. During hot pressing, the nitrogen is compressed. The subsequent sintering step then causes the compressed nitrogen to swell (see Fig. 5). Oxygen shows a different behavior. It is able to diffuse through the ceramic lattice described during hot pressing, as a result that the density remains almost constant with increasing sintering time.

Because of a lead oxide liquid phase of 1.5 mol%, matrix coarsening was calculated using the cubic growth law developed by Lay [14] (Eq. 1).

$$r^3 - r_0^3 = 1.05Kt \tag{1}$$

where r is the grain size measured after a particular sintering time t, r_0 the grain size directly after heating to sintering temperature, and K is a growth constant. Figure 2 shows the Lay-fit [14] of the measured grain size at 950 and 1150 °C. The calculated K-values used for the Lay-fit are displayed in Table 1. The calculated progression of grain coarsening at 950 °C corresponds well to the measured grain size of both PMN-32PT and PMN-37PT-21PZ. However, grain coarsening deviates from the predicted progression for sintering times higher than 2 h at 1150 °C. This saturation is consistent with the results of Sabolsky et al. [8]. Matrix coarsening leads to an increased liquid layer thickness δ [15] that causes longer diffusion lengths. Furthermore, the surface energy of coarse grains is reduced. Consequently, the solubility of the matrix is decreased, which leads to a lower grain growth rate. The difference between the measured grain size and the fitted Lay model can be explained by closer examining the growth constant K, which was also described in the Lay model [14] (see Eq. 2).

$$K = \frac{DS_0M\sigma}{RT\rho^2c} \tag{2}$$

where D is the diffusion constant, S_0 the average material solubility, M the molar weight, σ the surface energy, R the gas constant, T the temperature, and ρ is the density of the solid phase. The constant c is given by Eq. 3 [14].

$$c = \frac{\delta}{r} \tag{3}$$

where δ is the thickness of the liquid phase. Combining Eqs. 2 and 3 makes clear that the growth constant decreases if the liquid layer thickness increases. This means that if the same growth constant (as displayed in Table 1) is used for all sintering times, the difference between the calculated grain size and the measured grain size increases with increasing sintering time (>2 h). The use of a fixed growth constant is consequently restricted to short sintering times in the context of calculating grain size using the Lay model [14].

Single crystal growth of both PMN-32PT and PMN-37PT-21PZ matrices was fitted using a model of Seabaugh et al. [16] (see Eq. 4).

$$L_t - L_0 = 5.81K^{1/3}t^{1/3} + 1.48K^{2/3}\left[\frac{\rho RT}{M\sigma}(1 - k_{hkl})\right]t^{2/3} \tag{4}$$

where L_t is the single crystal growth that occurs after a particular sintering time t, L_0 the grain size directly after heating to sintering temperature, and k_{hkl} is a constant that

is dependent on the single crystal orientation. For the growth of PMN-PT single crystals in a PMN-PT matrix using a (001)-oriented BT seed single crystal, k_{001} was found to be 1 [17]. Using Eq. 4 and $k_{001} = 1$, the measured single crystal growth of both matrices was fitted (Fig. 5). For the investigated sintering times, no saturation of single crystal growth was observed. The measured single crystal growth decreases with increasing sintering times as predicted by the cubic growth law of Seabaugh et al. [16]. Because of the clear size advantage of the single crystal (infinite curvature), no saturation or deviation from the calculated single crystal growth was observed although a fixed growth constant was used.

The very high growth rates at the beginning of the growth of the (111) oriented single crystals will be reduced severely. The reason is the (111) growth front will eventually disappear leaving only the slower growing faces. This agrees with findings of Rehrig et al. [18].

The fact of a dense matrix caused a doubling of the single crystal growth length (Fig. 5 and Table 2). As already mentioned, one possibility to prevent porosity is to carry out a prior densification by hot pressing in oxygen. Figure 4 shows that hot pressing in oxygen can prevent porosity within the single crystal grown. This plays a crucial role for single crystal growth, because porosity reduces single crystal growth length as can be seen in Figs. 4 and 5. Gorzkowski et al. [6] have also reported the same (see Table 2). The reason for this is the lower mobility of pores relative to the growing single crystal layer [19]. At the beginning of the growing process, pores are small, which reduces the growth velocity only slightly [20]. Increased sintering time leads to pore coarsening, which clearly hinders single crystal growth via pore dragging. The development of pores can be observed in Fig. 4b and d. Pore size increases with increasing distance from the interface of the BT seed single crystal and the grown PMN-32PT single crystal.

Due to their dissolution into the PMN-32PT matrix, ST single crystals cannot be considered suitable for seeding. No single crystal growth was observed after 2 h at 700 °C (below the melting point of PbO). Instead of the expected single crystal, a Sr diffusion layer with a width of ~50 μm was formed (Fig. 6a). It is well known that Sr replaces Pb, and this is visible in the development of Sr and Pb within the Sr diffusion zone (Fig. 6a). Starting at the ST seed single crystal, the Sr content decreases and the Pb content increases gradually. BT seed single crystals, in contrast, are chemically stable (Fig. 6b). The different growth behavior of BT and ST single crystals can be attributed to differences in cation vacancies prevalent within the two different single crystal materials. It was shown for donor-doped ST that Sr vacancies prevail strongly over Ti vacancies [21]. Even in undoped ST, more than 2×10^{18} cm^{-3} doubly ionized Sr vacancies are present [22]. In strong contrast to ST, Ti vacancies prevail in BT [23]. Therefore, it becomes clear that in ST A-site cation interdiffusion is possible, at least at high sintering temperatures where the thermally activated diffusion coefficient of the A-site cations is high enough. This will eventually lead to the observed Sr and Pb diffusion profiles in Fig. 5. Since in BT cation diffusion goes over Ti-vacancies, no A-site interdiffusion is possible and the single crystals can grow in the matrix as it is the case for BT single crystals in Fig. 6a.

Conclusions

The aim of this study was to investigate single crystal growth behavior in PMN-32PT and PMN-37PT-21PZ. (001)- and (111)-oriented $BaTiO_3$ (BT) single crystals and (001)-oriented $SrTiO_3$ (ST) single crystals were used as seeds. Samples were densified by hot pressing in an air or in an oxygen atmosphere. During subsequent sintering of seeded samples, matrix coarsening takes place and single crystal growth occurs. The matrix grain growth observed was fitted using the Lay model [14]. It was shown that using an air atmosphere during hot pressing leads to a porous microstructure after subsequent sintering, whereas oxygen hot pressed samples maintain their dense microstructure even after sintering. The measured growth length of PMN-32PT and PMN-37PT-21PZ single crystals nucleated from (001) BT single crystal was up to 140 μm for

Table 2 Growth length of (001)-oriented single crystals in a dense, fine grained matrix and in a porous matrix

Matrix/(001) single crystal	PbO_{excess}/mol%	Single crystal growth $L_t - L_0$/μm	HP-atmosphere/ porosity	Reference
PMN-32PT/BT	1.5	140	Oxygen/no	Present work
		81	Air/yes	
PMN-37PT-21PZ/BT		65	Oxygen/no	
PMN-35PT/PMN-35PT	1.5	160	Vacuum/no	[6]
	1.5	115	Air/yes	[7]
PMN-35PT/BT	1	85	Air/yes	[8]
	3	115	Air/yes	

PMN-32PT and 65 μm for PMN-37PT-21PZ. Single crystal growth of the (001)-oriented single crystal of both compositions can be described using a cubic growth law mentioned by Seabaugh et al. [16]. The growth length of the (111) PMN-32PT single crystals nucleated from (111) BT single crystals was significantly higher than that of the (001) PMN-32PT single crystals nucleated from (001) BT single crystals. Single crystal growth of up to 1 mm was measured. Growth experiments using (001) ST seed single crystals failed due to the dissolution of ST into the PMN-32PT matrix. The differences between BT and ST as single crystals could have been explained by defect-chemistry.

Acknowledgement This work was supported by the German Federal Ministry of Education and Research under BMBF grant number 03X4001A.

References

1. Khan A, Meschke FA, Li T, Scotch AM, Chan HM, Harmer MP (1999) J Am Ceram Soc 82:2958
2. Xu Z, Chen F, Xi Z, Li Z, Cao L, Feng Y, Yao X (2004) Ceram Int 30:1777
3. Du XH, Zheng J, Belegundu U, Uchino K (1998) Appl Phys Lett 72:2421
4. Jaffe B, Cook WR Jr, Jaffe H (1971) Piezoelectric ceramics. Academic Press Inc., London
5. Richter T, Denneler S, Schuh C, Suvaci E, Moos R (2008) J Am Ceram Soc 91:929
6. Gorzkowski EP, Chan HM, Harmer MP (2006) J Am Ceram Soc 89:856
7. King PT, Gorzkowski EP, Scotch AM, Rockosi DJ, Chan HM, Harmer MP (2003) J Am Ceram Soc 86:2182
8. Sabolsky EM, Messing GL, Trolier-McKinstry S (2001) J Am Ceram Soc 84:2507
9. Li T, Wu S, Khan A, Scotch AM, Chan HM, Harmer MP (1999) J Mater Res 14:3189
10. Kwon S, Sabolsky EM, Messing GL, Trolier-McKinstry S (2005) J Am Ceram Soc 88:312
11. Khan A, Carpenter DT, Scotch AM, Chan HM, Harmer MP (2001) J Mater Res 16:694
12. Kwon S, Sabolsky EM, Messing GL (2001) J Am Ceram Soc 84:648
13. Cho SJ, Kang SJL, Yoon DN (1986) Metall Trans A 17:2175
14. Lay KW (1968) J Am Ceram Soc 51:373
15. Hennings DFK, Jannsen R, Reyen PJL (1987) J Am Ceram Soc 70:23
16. Seabaugh M, Suvaci E, Brahmaroutu B, Messing GL (2000) Interface Sci 8:257
17. Messing GL, Trolier-McKinstry S, Sabolsky EM, Duran C, Kwon S, Brahmaroutu B, Park P, Ylmaz H, Rehrig PW, Eitel KB, Suvaci E, Seabaugh M, Oh KS (2004) Crit Rev Solid State Mater Sci 29:45
18. Rehrig PW, Messing GL, Trolier-McKinstry S (2000) J Am Ceram Soc 83:2654
19. Nicholson FA (1968) J Am Ceram Soc 51:468
20. Brook RJ (1969) J Am Ceram Soc 52:567
21. Moos R, Bischoff T, Menesklou W, Härdtl KH (1997) J Mater Sci 32:4247. doi:10.1023/A:1018647117607
22. Moos R, Härdtl KH (1995) J Am Ceram Soc 78:2569
23. Moos R, Härdtl KH (1997) J Am Ceram Soc 80:2549